J Comp Physiol A (1992) 171:421–435

Journal of Comparative Physiology A Sensory, Neural, and Behavioral Physiology

Diversity of form in the amphibian papilla of Puerto Rican frogs

Edwin R. Lewis[1], Eva I. Hecht[1] and Peter M. Narins[2]

[1] Electronics Research Laboratory, University of California, Berkeley, CA 94720, USA
[2] Department of Biology, University of California, Los Angeles, CA 90024, USA

Accepted June 18, 1992

Summary. In modern frogs, the amphibian papilla exhibits a caudal extension whose shape, relative length, and proportion of hair cells vary markedly from species to species. Tuning in the caudal extension is organized tonotopically and evidently involves the tectorium. In terms of the proportion of amphibian-papillar hair cells in the caudal extension, we report more diversity among 8 species of a single genus *(Eleutherodactylus)* on a single island (Puerto Rico) than has been found so far among all of the (more than 50) other modern anurans examined for this feature from around the world. These 8 Puerto Rican species have overlapping habitat and conspicuous diversity in the male advertisement call. For 7 of the 8 species, we report that the call has transient spectral components in the frequency range of the amphibian papilla, and that the proportion of caudal extension hair cells and the frequency distribution of those components are correlated. Thus one might conclude that the selective pressures that led to diversity of calls among the 8 species also led to diversity in form of the amphibian papilla.

Introduction

The amphibian papilla, one of at least 4 acoustic sensors in the frog ear[1], resides on the ceiling of a separate chamber of the inner ear (Retzius 1881; Geisler et al. 1964; Wever 1973, 1985; Capranica 1976; Lewis 1976, 1981, 1984). In neobatrachian (modern) frogs, the amphibian papilla (AP) comprises 3 distinct regions (denoted A, B and C in Fig. 1). Whereas the relative lengths of regions A and B and the relative numbers of hair cells contained in them are fairly constant among these frogs, those of region C (the caudal extension) are extremely variable – suggesting considerable susceptibility to selective pressures (Lewis 1984; Lewis and Lombard 1988). In neobatrachians considered to be most derived (on the basis of character traits not related to the ear – Lynch 1971; Duellman 1975), the caudal extension usually is so elongated that it reaches beyond the caudalmost end of the AP chamber ceiling and curves well down the wall at that end. In this project, we explored the amphibian papillae of Puerto Rican (PR) frogs of a single genus, *Eleutherodactylus*. What we found among 8 species of that one genus (considered highly derived – Lynch 1971) on that one island, was a far greater range of variability in the proportion of hair cells in the caudal extension than we had seen in any other anuran group. We also

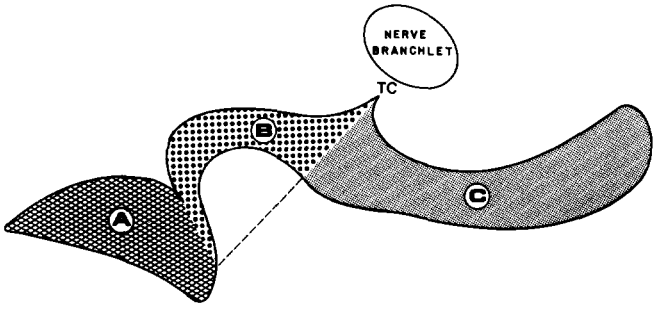

Fig. 1. Outline of an amphibian papilla from the left ear of a neobatrachian (modeled after *E. hedricki*). Anterior is on the left, lateral on the top. The papilla comprises two patches, one designated region *A*, the other designated regions *B* and *C* (C being the caudal extension of the papilla). The boundary between regions A and B is punctuated by a local gradation in hair bundle shape and an abrupt change in hair bundle orientation (Lewis et al. 1982b). A line from the tectorial corner *(TC)* to the anteromedial end of region B divides regions B and C. This line corresponds to the position of the diaphragm (see Figs. 7 and 8). In region B, the hair bundles have longitudinal orientation; in region C they have transverse orientation

Abbreviations: *AP* amphibian papilla; *BEF* best excitatory frequency; *PR* Puerto Rican; *SEM* scanning electron microscope; *SVL* snout-vent length; *TC* tectorial corner; *TM* tectorial membrane

Correspondence to: Prof. E.R. Lewis

[1] The other acoustic sensors are the basilar papilla (which covers a frequency range above that of the AP), the sacculus (which covers a frequency range below that of the AP), and the lagena (which is partly an acoustic sensor, partly an equilibrium sensor)

found evidence of sexual dimorphism in one species (*E. coqui*); in the female of that species we found the highest proportion of hair cells in the caudal extension that we have seen in any frog (76 species examined). Subsequently, we analyzed recorded advertisement calls from the males of these species and, for several of them, found correspondences between transient spectral components of the calls and the proportion of hair cells in the caudal extension. In this paper, we present what we consider to be the essential details of these results and their implications regarding function. From these, we move to a speculative discussion about the selective advantages of the caudal extension and about the involvement of the tectorial membrane in the tuning of that structure. A preliminary presentation of some of these results appeared in Lewis and Lombard (1988).

Hanging from the AP, the acellular tectorial membrane is bulky under region A, filling almost completely the rostral end of the AP chamber, and thin under regions B and the caudal extension (C), filling less than half of the volume of that part of the chamber. In Fig. 1, the boundary between region B and the caudal extension, denoted by the dashed line, corresponds to the position of a thin diaphragm (part of the tectorial membrane) that spans the papillar chamber and is firmly connected on all sides – to microvilli on the chamber wall and to the rest of the tectorial membrane. In the caudal extension of neobatrachian frogs, the polarization axes[2] of the hair bundles are oriented perpendicular to the edges of the papilla (i.e., transverse to the curved, long axis of the papilla); in region B they are oriented parallel to the edges of the papilla (longitudinal with respect to the long axis of the papilla) (Lewis 1976, 1984). In light of the observation that the hair cell is most sensitive to bundle displacements directed along the polarization axis (Lowenstein and Wersäll 1959; Flock 1965; Hudspeth and Corey 1977), the difference in polarization between the bundles in region B and those in the neobatrachian caudal extension could be assumed to reflect a difference in the direction of motion of the tectorial membrane in the two regions in response to acoustic stimuli. The transition from transverse to longitudinal motion would occur in the immediate vicinity of the diaphragm.

Based on their tuning properties, which have been observed in many species of neobatrachian frogs, frog auditory axons consistently can be divided into 3 groups: a group of (supressible) low-frequency axons (BEFs ranging approximately from 100 to 600 Hz) that exhibit two-tone suppression; a group of (non-supressible) midfrequency axons (BEFs ranging approximately from 450 to 1000 Hz) that do not exhibit two-tone suppression; and a group of non-supressible high-frequency axons (BEFs ranging approximately from 1400 Hz to 4 kHz, depending on the species) (Frishkopf and Goldstein 1963; Sachs 1964; Frishkopf and Geisler 1966; Feng et al. 1975; Capranica and Moffat 1974a, b, 1975; Hillery and Narins 1987; Zakon and Wilczynski 1988). In *Rana catesbeiana*, and presumably in all frogs, the high-frequency axons arise from the basilar papilla (Feng et al. 1975; Lewis et al. 1982a). In frog species in which adults are small, the BEFs of high-frequency axons often have been found to correspond to the dominant spectral components of the male's advertisement calls (Zakon and Wilczynski 1988).

Low- and midfrequency axons arise from the AP (Feng et al. 1975). Among the 4 species examined by Capranica and his colleagues (Capranica and Moffat 1974b, 1975; Feng et al. 1975; Capranica 1976) in their first studies of these axons, the proportion of axons falling into the non-supressible midfrequency class varied markedly, from 0 in *Scaphiopus couchi* to 17% in *Bufo debilis* to 37% in *Bufo americanus* to 50% in *R. catesbeiana*. SEM studies revealed that these proportions corresponded almost precisely to the proportions of AP hair cells located in the caudal extensions of those animals (Lewis 1977). Thus, we have the strong implication that non-supressible midfrequency axons innervate the (transversely-oriented) hair cells of the neobatrachian caudal extension; supressible axons innervate regions A and B. This was verified subsequently by combined physiology and intracellular marking in *R. catesbeiana* (Lewis et al. 1982b).

BEFs vary from one non-supressible midfrequency axon to another. In neobatrachian species they range over approximately 0.5 to 1.5 octaves (depending on the species). In *R. catesbeiana*, and presumably in the other neobatrachian species, the caudal extension is organized tonotopically, along the long axis of the papilla. Axons with lowest BEFs (approximately 450 Hz) arise near the diaphragm and axons with highest BEFs (approximately 1000 Hz in *R. catesbeiana*) arise from the caudal-most end of the papilla.

Eleutherodactylus presently ranks as the most speciose vertebrate genus, with 398 named species and many evidently remaining to be named (Lynch and Myers 1983; Duellman and Trueb, 1985; Hanken 1989). The distribution extends from Mexico to northern Argentina and southern Brazil, and includes the West Indies (Lynch 1971). On the island of Puerto Rico there are 15 species, 13 being endemic and 2 being shared with the Virgin Islands (Schwartz and Henderson 1985). Two of the Puerto Rican (PR) species (*E. unicolor* and *E. richmondi*) are fossorial and do not possess the large digital pads typical of arboreal frogs. One PR species (*E. karlschmidti*) is aquatic and possesses fully-webbed hind feet – an unusual trait in this genus, and a double vocal sac. The remaining twelve PR species of *Eleutherodactylus* have large digital pads and no webbing; color and size are the principal morphological features used to distinguish them from one another (Schwartz and Henderson 1985). Each of the 15 PR species, however, has its own highly-distinctive advertisement call (Rivero 1978; Drewry and Rand 1983).

Among the published spectrograms for the calls of the 8 species we studied, only those for *E. coqui* and *E. portoricensis* showed significant energy in the frequency range of the AP (i.e., 100 to 1400 Hz) (Drewry and Rand 1983). For the other species, the energy appeared to be confined

[2] The polarization axis is defined to be a line in the plane of the luminal surface of the hair cell, parallel to the gradient of stereocilia length

to basilar-papillar frequencies. Therefore, after making our morphological observations, we carried out detailed analyses of the vocalizations of the 8 species, searching for subtle components that would excite the AP.

Materials and methods

Eight species were used in this study. *E. antillensis, E. hedricki, E. richmondi* and *E. wightmanae* all were taken at the El Verde Field Station of the University of Puerto Rico. *E. brittoni* was taken at low elevations in the Luquillo Mountains; *E. coqui* and *E. portoricensis* were taken at high elevations in the same mountains. *E. cooki* was taken in caves in the Sierra de Panduras of southeastern Puerto Rico. All but 4 of the animals used in this study were adult males. This was a consequence of the fact that specimens usually were located by their advertisement calls, and only the adult males call. Noncalling adult males of *E. richmondi* and *E. hedricki* were captured by M.M. Stewart and her coworkers and given to us for this project. Two *E. coqui* were females and one *E. cooki* was a female, another a subadult male. The animals were identified by their calls, when available, and by external morphological features – principally color patterns (see Rivero 1978; Schwartz and Henderson 1985).

Each animal was given a large overdose of sodium pentobarbital (intraperitoneal). As soon as the anesthetic had taken effect, the animal was decapitated and the lower jaw was removed. Through the roof the mouth the bony capsule of the ear was opened by gentle shaving with a sharp scalpel. The head then was immersed in 2% glutaraldehyde in 0.2 *M* sodium cacodylate buffer, pH 7.4, and stored at 4 °C. The rest of the animal was preserved in 10% formalin (with saturated magnesium carbonate) as a voucher specimen. After at least 48 h of fixation in glutaraldehyde, the head was rinsed for 15 min in 0.2 *M* sodium cacodylate buffer. Then the membranous labyrinths were removed from the bony capsule and placed in 1% osmium tetroxide solution in 0.2 *M* sodium cacodylate buffer. After 1 h of postfixation in the osmium solution, the labyrinths were rinsed for 15 min in sodium cacodylate buffer and then dissected free hand, with a fresh razor blade. The APs were removed and placed in fresh buffer for temporary storage (at 4 °C). The AP tectorial membranes were retrieved and stored separately in fresh buffer.

The APs were dehydrated through a graded series of ethanol/water mixtures, with 3 repetitions at 100% ethanol. Then they were transferred to a pressure bomb, and the ethanol was replaced by liquid carbon dioxide. The tissues were dried by the critical-point method, mounted on a viewing stub, and sputter coated with a very thin layer of gold. The coated specimens were viewed and photographed in an AMRay 1000A scanning electron microscope. The AP tectorial membranes were transferred by pipette, in buffer, to the wells of depression slides. The wells were covered with number 1 cover slips, and the material viewed and photographed in the wet state with a Zeiss Universal laboratory microscope.

Calls of *E. brittoni, E. cooki, E. hedricki, E. richmondi* and *E. wightmanae* all were transcribed from the published recordings of Rivero (1978). Those of *E. antillensis, E. coqui* and *E. portoricensis* were recorded in the field on a reel-to-reel recorder (Stellavox SP8: 30–20000 Hz), with a directional microphone (AKG CE8). Transcribed or recorded calls were analyzed by being passed through analog electronic band-pass filters (Krohn-Hite model 3343) spanning various parts of the AP frequency range (e.g., the octaves 100–200 Hz, 200–400 Hz, 400–800 Hz, and the half-octaves 800–1100 Hz and 1100–1600 Hz). The filters were 16 pole, Butterworth configurations, with 48 dB/oct asymptotic slopes on the low- and high-frequency sides. The (unaveraged) outputs from the filters were captured in precise synchrony by means of a digitizing oscilloscope (Hewlett-Packard model 54501A) and examined for quasi-steady-state responses and for transient responses to individual calls.

Results

Hair cell counts

Compared with that of the other modern frogs we have studied, the caudal extensions in the 8 species of *Eleutherodactylus* were proportionately longer and extended

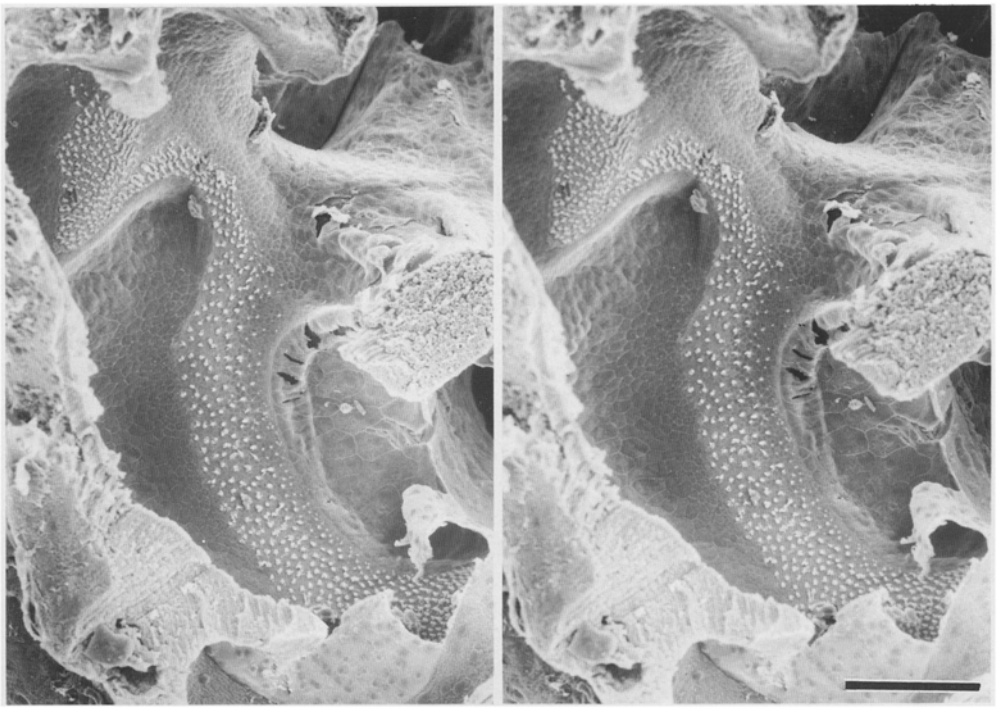

Fig. 2. Stereo scanning electron micrograph of the amphibian papilla (and environs) from the left ear of a male *E. coqui*. Horizontal bar = 100 μm. Here we are viewing the dorsal wall of the papillar chamber from below. The sensory surface, dotted with hair bundles, is integrated into the ceiling and posterior wall of the chamber. At the posterior end of the chamber it is partially obscured by remnants of the contact membrane, which separated the chamber from the periotic canal in the intact ear

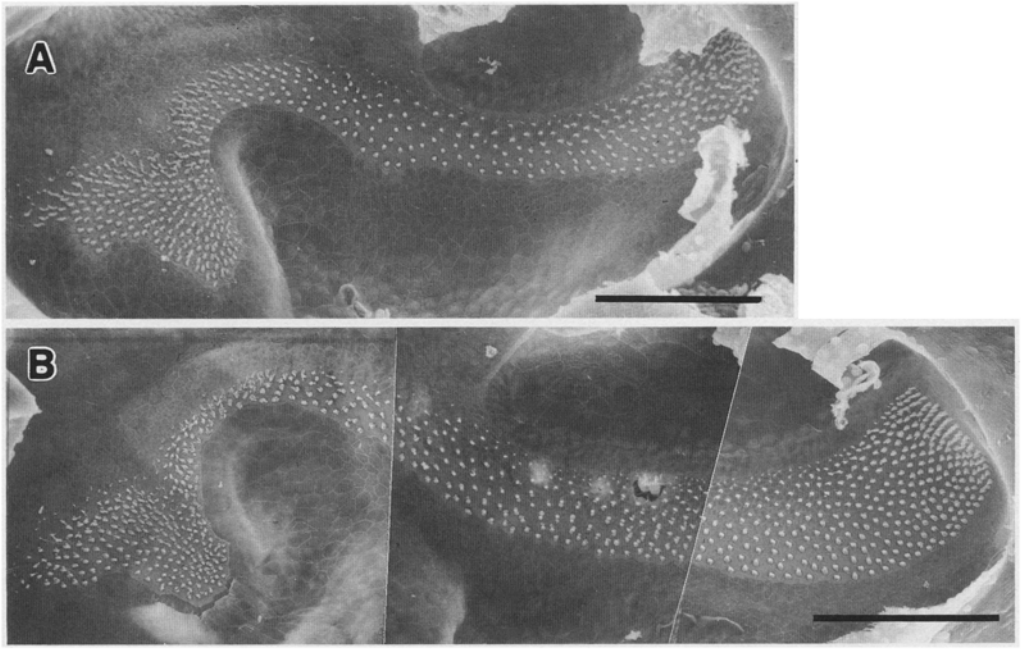

Fig. 3A, B. Scanning electron micrographs of amphibian papillae from the left ears of two Puerto Rican species of the genus *Eleutherodactylus*, viewed from below. **A** *E. wightmanae*; **B** *E. richmondi*. Horizontal bars = 100 μm. The papillar sensory surfaces are dotted with the hair bundles of the receptor cells (hair cells)

Table 1. Hair-cell counts for the amphibian papillae of 8 Puerto Rican species of the genus *Eleutherodactylus*

Subject	Species	Side	Hair Cells Region A	Hair Cells Region B	Hair Cells Caud Ext	SVL (mm)
1	*antillensis*	L	134	150	379	22
	antillensis	R	155	135	354	22
2	*antillensis*	L&R	157(L)	136(L)	415(R)	22
3	*brittoni*	L&R	167(L)	143(L)	226(R)	15
4	*cooki* (juv.)	R	187	172	400	32
5	*cooki*	L	214	193	499	43
	cooki	R	208	182	471	43
6	*coqui*	L	171	196	520	43
7	*coqui*	L	195	228	510	47
8	*coqui* (fem.)	L	181	196	650	60
9	*coqui* (fem.)	L	150	176	593	55
	coqui (fem.)	R	156	178	607	55
10	*hedricki*	L	207	191	267	29
11	*portoricensis*	L	172	173	424	33
	portoricensis	R	187	178	459	33
12	*portoricensis*	L	187	166	414	25
	portoricensis	R	183	155	369	25
13	*portoricensis*	R	157	127	307	36
14	*richmondi*	L	196	158	549	24
15	*wightmanae*	L	181	162	401	16
	wightmanae	R	210	161	409	16
16	*wightmanae*	L	141	129	254	16

proportionately farther down the posterior wall of the AP chamber. An example of the resulting bending of the papilla can be seen in the stereomicrograph of the AP of a male *E. coqui* in Fig. 2. This bending made dissection difficult, especially with the smaller species. Because the bend occurs in the middle of the caudal extension, it also made accurate measurement of the length of that part of the AP very difficult. Therefore, for these comparative studies we elected to focus on hair-cell counts rather than lengths. Our intention was to compare the numbers of hair cells in regions A, B and the caudal extension among the 8 species. In order to obtain the hair-cell counts, we needed to expose entire, intact papillae. This required removal of the entire ventral wall of the chamber while leaving the dorsal and posterior walls unscathed. In several species (especially *E. antillensis, E. brittoni* and *E. wightmanae*) our success rate was low. Typically, either the caudalmost or rostralmost end of the papilla was

blocked from view by residual ventral-wall tissue, or the caudalmost end of region C had been nicked by the razor blade – in either case making accurate hair cell counts impossible. For the purpose of this project, we intended to use only those papillae that were both intact and adequately exposed for complete hair-cell counts. For *E. brittoni* we failed to obtain such specimens. We did obtain intact and exposed regions A and B (with part of the caudal extension) from the left ear of a subject and intact and exposed caudal extension (plus part of B) from the right ear of the same subject. Therefore, for that species, we used composite data. We did the same thing for one *E. antillensis* subject. The remaining data were taken from papillae that were intact and completely exposed. The latter often required photomicrographs taken from several angles, however. Two examples of succesfully dissected papillae are shown in Fig. 3. Our data, displayed in Table 1, were taken from twenty intact papillae (from fourteen subjects) and two composite papillae.

Although the snout-vent lengths (SVL) of the subjects in Table 1 exhibited a 4:1 range, the hair-cell counts in regions A and B exhibited ranges of only 1.6:1 and 1.7:1, respectively. The hair-cell counts in the caudal extensions exhibited a range of 2.9:1. Thus, in terms of hair-cell counts, the caudal extension exhibited considerably more variability than did regions A and B. Because we were interested in the relative number of hair cells in the caudal extension, we divided the counts for that region by those for regions A and B, producing two morphological indices for each papilla (C/A = number of hair cells in the caudal extension divided by number of hair cells in A; C/B = number of hair cells in the caudal extension divided by number of hair cells in B). Figure 4 is a scatter diagram of the 20 intact papillae and two composite papillae plotted with C/A as one axis and C/B as the other. Smooth boundaries have been drawn around the datum points for species for which more than one papilla was available, with separate boundaries for males and females of *E. coqui*. The compactness of the areas enclosed in these boundaries is evidence of the appropriateness of our choice of morphological indices. A smooth boundary also has been drawn around the entire data set.

In Fig. 5, this overall boundary is compared with those obtained in the same way for a total of 58 species from other groups. Here the ranid frogs are represented by 8 species from the genus *Rana;* the intermediate frogs are represented by 16 bufonids, 15 species of *Bufo* and 1 *Atelopus*), 2 dendrobatids (both of the genus *Dendrobates*), four microhylids (2 species of *Gastrophryne* and 1 each of *Hypopachus* and *Kaloula*), and 14 hylids (7 species of *Hyla,* 2 each of *Acris* and *Pseudacris,* and 1 each of *Phrynohyas, Pternohyla,* and *Smilisca*); the ancient frogs are represented by 3 discoglossids (2 species of *Bombina* and 1 of *Alytes*), 4 pipids (3 species of *Xenopus* and 1 of *Pipa*), and 6 pelobatids (5 species of *Scaphiopus* and 1 of *Pelobates*) (see Lewis 1984). Table 2 shows examples of AP hair cell counts from 26 of these other species (all 8 species from *Rana* plus all anuran species for which AP hair-cell counts were made by both

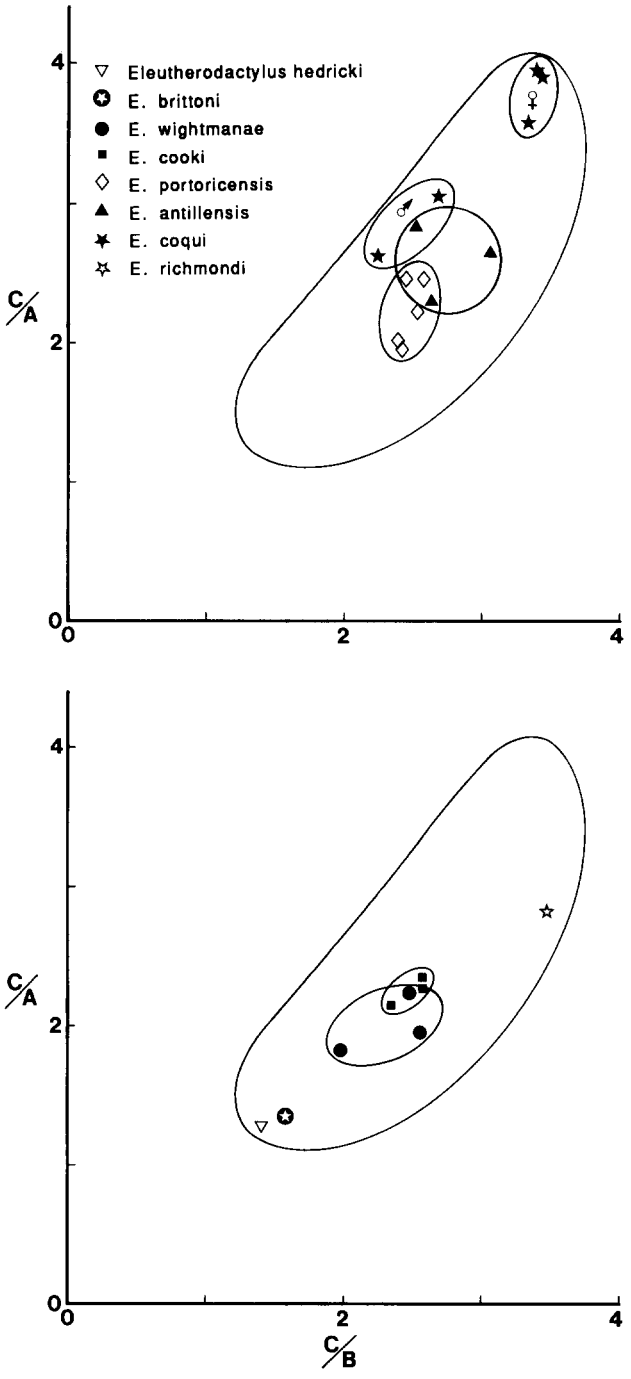

Fig. 4. Diversity of the AP caudal extension in 8 Puerto Rican species of the genus *Eleutherodactylus*. Scatter diagram of 20 intact amphibian papillae and 2 composite amphibian papillae plotted over 2 morphological indices. *A, B* and *C* are the numbers of hair bundles counted in regions A, B and C (caudal extension)

Wever (1985) and us). With respect to the chosen indices of AP morphology, Fig. 5 shows as much diversity among individuals of some PR *Eleutherodactylus* species as it does among the 8 species of *Rana* (selected randomly, on the basis of availability from suppliers and colleagues: *boylei, cascadae, catesbeiana, clamitans, palustris, pipiens, sylvatica,* and *utricularia*). In Fig. 5, the total range of diversity of AP morphology for the 20 papillae and 2 composites from PR *Eleutherodactylus* frogs is

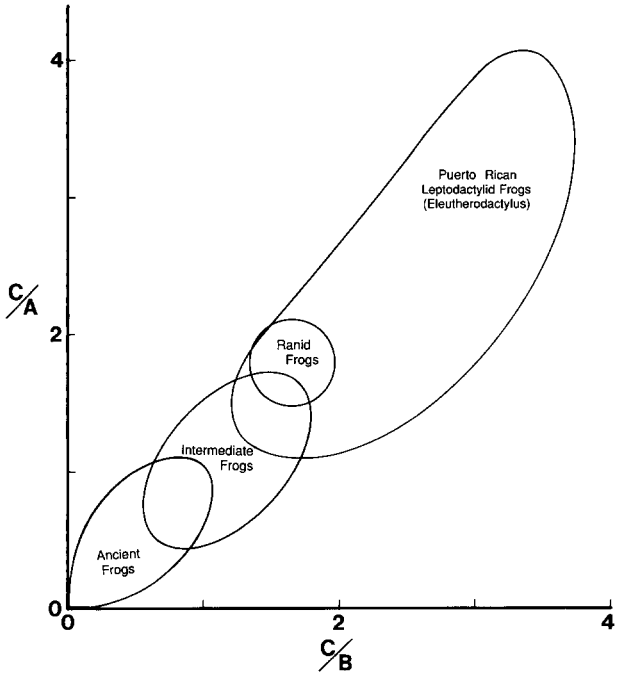

Fig. 5. Boundaries of the C/A vs. C/B datum points for 8 Puerto Rican *Eleutherodactylus* frogs compared with the boundaries for 3 other groups of frogs (a total of 58 comparison species). The boundaries for ranid, bufonid, and ancient frogs were smooth curves that enclosed all data points without margins of error

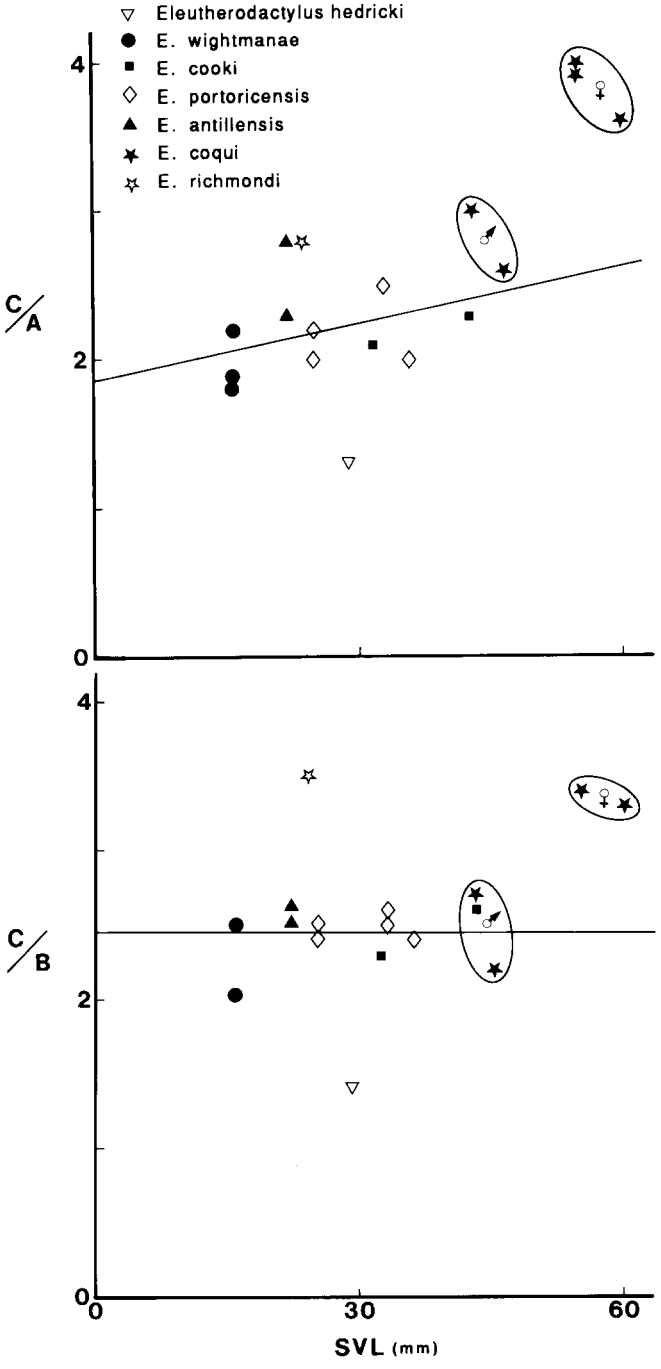

Fig. 6. Tests for dependence of the indices of Figs. 4 and 5 on frog size. *SVL* = snout-vent length. The elliptic boundary on the upper right in each diagram surrounds the datum points for *E. coqui* females; the other elliptic boundary surrounds datum points for males of that species. The lines are linear regressions computed from all datum points except those of the *E. coqui* females

greater than that of all 58 comparison species taken together.

Although the sample is small (2 males, 2 females), the scatter diagram (Fig. 4) suggests sexual dimorphism in the ear of *E. coqui*. Male *E. coqui* are conspicuously smaller than females, however. To test the possibility that the morphological differences between the male and female *E. coqui* in our sample might be consequences of size difference, we plotted scatter diagrams of C/A and C/B vs snout-vent length (SVL) for the animals in our sample (Fig. 6). Linear regression lines for these data (excluding the female *coqui* papillae) show slight dependence of C/A on SVL [b_0(intercept) = 1.857; b_1(slope) = 0.0139; s_e(residual standard error) = 0.406; r(correlation coefficient) = 0.339], and virtually no dependence of C/B on SVL [$b_0 = 2.441$; $b_1 = 0.0006$; $s_e = 0.421$; $r = 0.015$]. In each plot, the data for female *E. coqui* are distinct outliers (approximately 2.5 standard errors from the regression line) and those for male *E. coqui* are not, suggesting that the differences between male and female papillae in this case are related to sex rather than size. This matter should be pursued with a focused study and larger samples.

Tectorial membranes

We examined tectorial membranes from *E. antillensis*, *E. brittoni*, *E. coqui*, *E. cooki* and *E. richmondi*. In terms of the morphological details described here, we found no obvious differences among these species. The tectorial membranes (TMs) shown in Figs. 7 and 8 are representative. That of Fig. 7 is from the right ear of a female *E. coqui* (subject 9 in Table 1) and is viewed dorsal-side up, directly toward the medial side. The sharply delineated upper edge of the TM corresponds to the boundary between the TM and the sensory surface (i.e., the place where hair cells contact the TM). The large tectorial mass that lies beneath AP region A is on the left; the portion of TM that lies beneath region B is largely out of focus

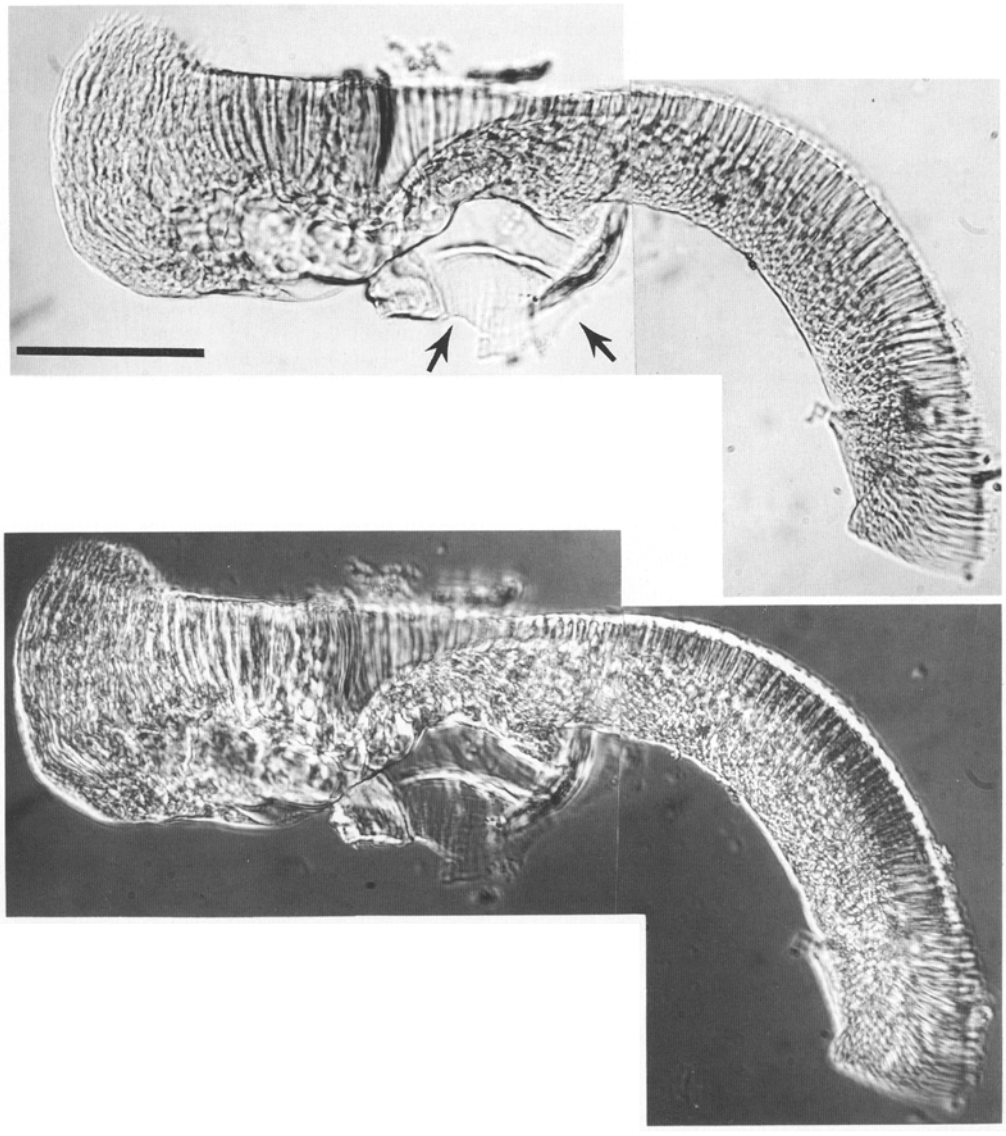

Fig. 7. Phase-contrast images of the AP tectorial membrane of the right ear of *E. coqui* (female, subject 9 in Table 1), viewed directly from its medial side. Anterior is on the left, dorsal on the top. Two *arrows* point to the diaphragm of the tectorium (also known as the tectorial curtain or sensing membrane). Horizontal bar = 100 μm. The upper micrograph was presented in Lewis and Lombard (1988)

in the center; and the portion associated with the caudal extension is on the right (approximately half of total apparent length of TM in these micrographs). Part of the diaphragm that spans the AP chamber appears in the center of each micrograph. The shape of right-hand end of the TM conforms to the curving of the papilla down the posterior wall of the AP chamber. This illustrates the reason dissection of the AP was difficult in the PR *Eleutherodactylus*.

Figure 8 shows TMs from the right ears of *E. antillensis* (subject 2 in Table 1) and *E. cooki* (a female in which accurate hair cell counts could not be obtained). The TMs are viewed toward their ventral sides. The surface of the TM that was directly in contact with the papilla is dark. The lighter regions extended beyond the papillar boundaries. For region A and part of region B, the lower micrograph is focused on the dorsal surface of the papilla (the surface farthest from the viewer), and clearly shows the pores that overlie the hair cells (one pore per hair cell). These pores evidently open into a system of channels that occur throughout the TM (see Wever 1985). In the TM layer closest to the papillar surface, the channels are perpendicular to that surface (particularly evident in Fig. 7). Adjacent to region B and the caudal extension, in the TM layer farthest from the AP surface, the channels tend to be parallel to the surface and perpendicular to the long axis of the AP (i.e., transverse). These transverse channels can be seen end-on in the micrographs of Fig. 7. Their orientation is more obvious in the lower micrograph of Fig. 8, which is focused on the transverse-channel layer beneath the caudal extension. The upper micrograph in Fig. 8 is focused on the ventral surface of the TM (the surface farthest from the AP and the hair cells). The tectorial diaphragm is clearly visible here, extending from the tectorial corner (lower right) to the base of region A (upper left).

Calls

Presently, the issue of how to describe isolated, transient waveforms (such as the acoustic waveform of a frog call)

Table 2. Hair-cell counts for the amphibian papillae of miscellaneous frogs and toads

Species	Hair Cells Region A	Hair Cells Region B	Hair Cells Caud Ext	C/A	C/B	Wever data ATB/SM/FS/PTB
Rana sylvatica	142	139	262	1.9	1.9	NA
R. boylei	216	219	344	1.6	1.6	NA
R. cascadae	167	170	316	1.9	1.9	NA
R. catesbeiana	300	377	582	1.9	1.5	537/239/17/381
R. pipiens	174	214	419	2.4	2.0	NA
R. utricularia	236	277	476	2.0	1.7	NA
R. clamitans	175	266	390	2.2	1.5	279/75/20/211
R. palustris	210	273	421	2.0	1.5	NA
Bufo alvarius	197	209	169	0.9	0.8	206/89/87/69
B. americanus	154	94	118	0.8	1.3	163/83/104/19
B. boreas	216	170	154	0.7	0.9	221/83/103/105
B. cognatus	98	90	87	0.9	1.0	163/106/22/113
B. marinus	244	173	220	0.9	1.3	244/146/5/230
B. valliceps	159	145	182	1.1	1.3	220/119/11/128
B. viridus	179	160	114	0.6	0.7	263/80/66/59
Hyla cinerea	133	175	212	1.6	1.2	191/69/12/392
H. versicolor	128	74	110	0.9	1.5	139/78/5/80
Acris crepitans	128	108	132	1.0	1.2	141/94/–/120
Gastrophryne olivacea	159	134	102	0.6	0.8	197/61/12/65
G. carolinensis	200	148	208	1.0	1.4	205/88/23/142
Kaloula pulchra	195	278	201	1.0	0.7	322/190/36/247
Bombina orientalis	183	173	0	0	0	205/92/68/0
B. bombina	127	128	33	0.3	0.3	208/70/64/0
Xenopus laevis	137	218	132	1.0	0.6	267/115/116/0
Pipa pipa	68	187	0	0	0	107/30/39/0
Scaphiopus hammondi	102	120	85	0.8	0.7	183/147/28/0

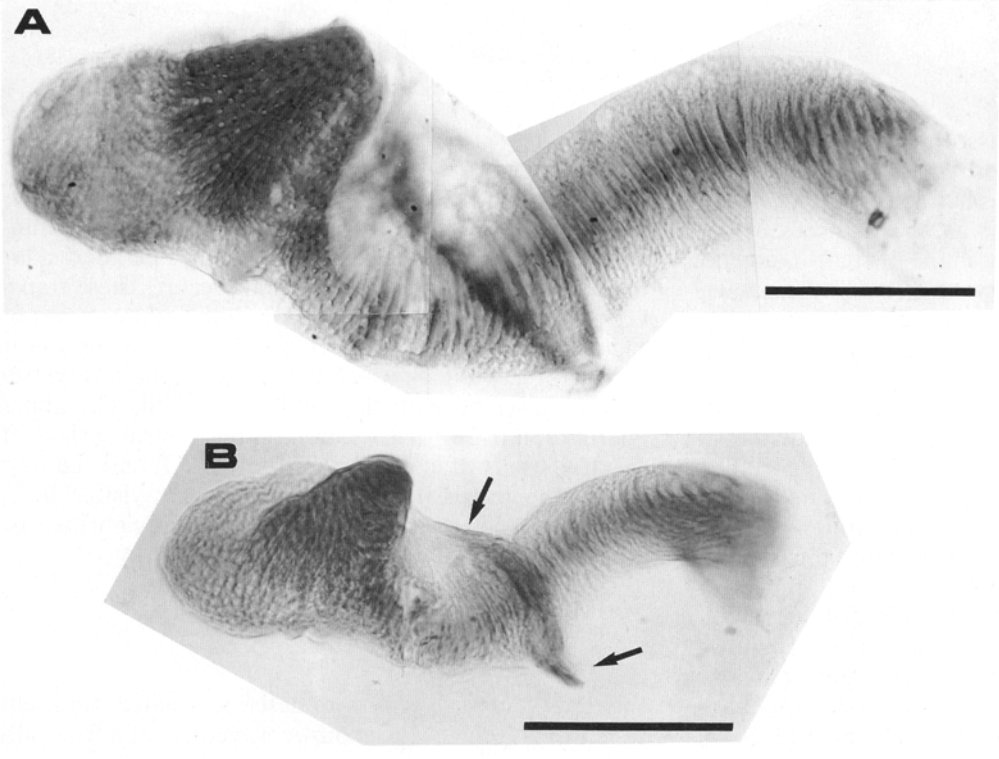

Fig. 8. Phase-contrast micrographs of AP tectorial membranes from the right ears of *E. cooki* **(A)** and *E. antillensis* **(B)**, viewed directly from their ventral sides. Anterior is the left, lateral on the bottom. Two *arrows* point to the diaphragm. Horizontal bar = 100 μm

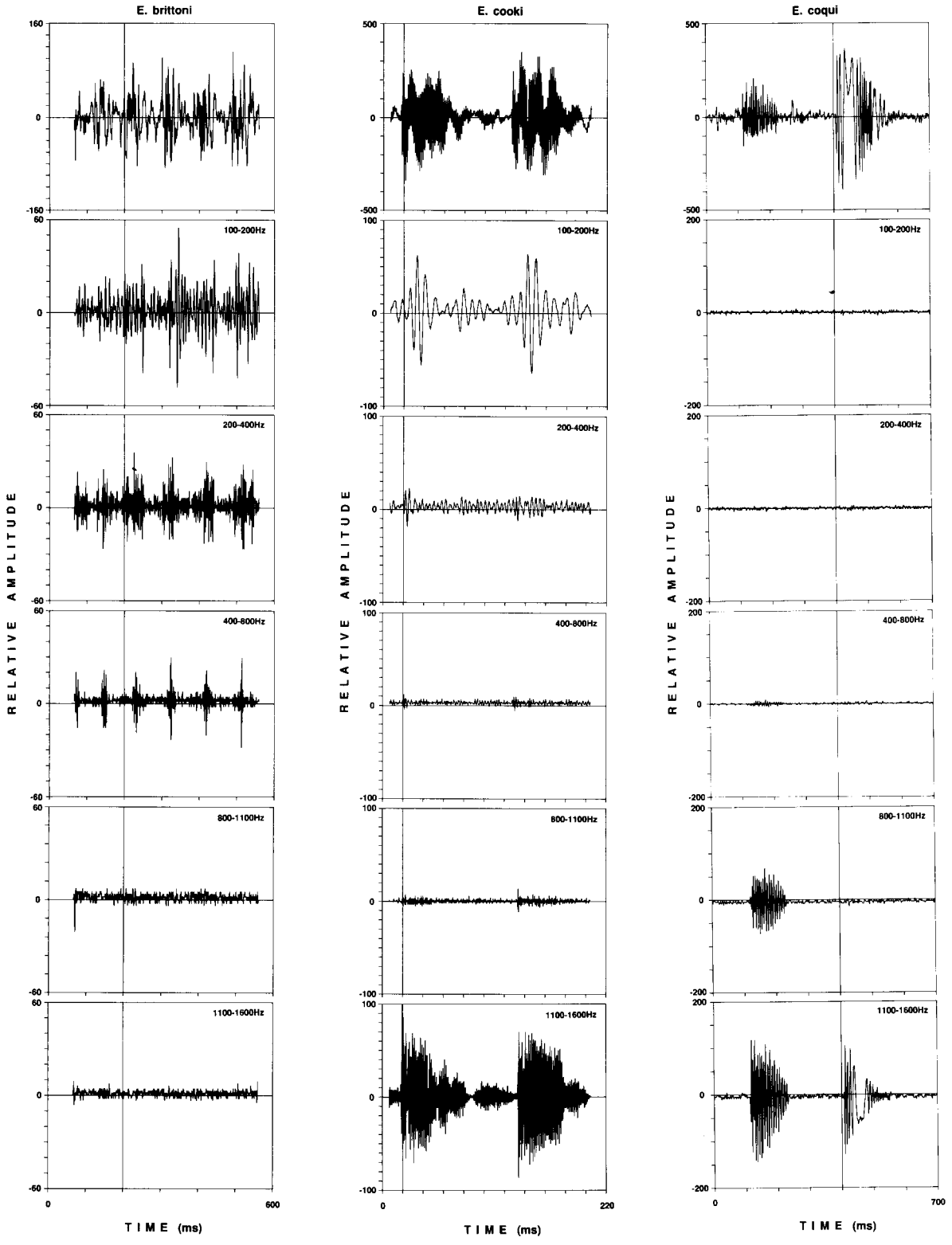

Fig. 9. Spectrographic analyses of advertisement calls of 3 species of *Eleutherodactylus*. Each trace was recorded on a digital storage oscilloscope. The top trace in each column is the unfiltered call. The traces beneath it are the responses of 16-pole band-pass Butterworth filters, the passbands of which are given in the upper right-hand corners of the boxes. The vertical line in each box corresponds to the time of triggering of the oscilloscope. For each species, the trigger was synchronized to the same phase of the unfiltered call for all traces. It is not always easy to distinguish particular responses from singularity responses. The response at the onset of the call in the 200–400 Hz passband for *E. cooki* is almost certainly a singularity response; the responses in the 1100–1600 Hz passbands for *E. cooki* and *E. coqui* are almost certainly particular responses

in terms of both frequency and time has not been resolved (Yen 1987; Cohen 1989). A common approach is spectrographic analysis, in which the waveform is applied to the inputs of an array of filters connected in parallel. Commonly each filter is characterized (in terms of its sinusoidal steady-state response) as having a certain frequency pass band, and the array of filters is taken to decompose a given frequency range into a set of contiguous bands. Thus, the set of filter responses to the waveform is taken to be a spectral decomposition of the waveform. Although acknowledged to be imprecise (strictly speaking, a transient waveform does not have a spectral decomposition) this scheme nonetheless usually is consistent and useful. For linear filters, such as those used in the spectrographic analysis of this study, the response waveform that actually emerges from each filter comprises the sum of two fundamentally different sets of components – a set of components whose shapes are determined by the filter itself and are the same for all transient input waveforms, and a set of components whose shapes are determined entirely by the input waveform. Because the latter correspond to the particular solutions of the differential equation describing the filter output when the waveform in question is applied to the input, they can be called particular responses. The former are evoked when (and only when) the input waveform exhibits a singularity (i.e., a stepwise change in amplitude or in any time derivative of amplitude) and therefore can be called singularity responses (see Fig. 10 for examples of singularity responses). Each waveform that begins in finite time (i.e., has not existed forever) or otherwise changes its trajectory from that which could be predicted from (noise-free, infinite bandwidth) observation of its immediate history has a singularity at the instant of the new trajectory's beginning.

Whenever responses (singularity responses, particular responses, or both) appear at the output of a filter, that conventionally is interpreted to imply that the input waveform has spectral components within the passband of the filter. Even with sinusoidal steady state, where spectral decomposition is valid, this interpretation is weakened by the fact that filter band edges have finite slopes at finite frequencies. Nevertheless, it is a satisfying interpretation because it generally is self-consistent – in the following senses: (1) Filters with similar passbands tend to produce singularity responses of similar amplitude when excited by the same transient waveform. (2) Filters with similar passbands and steep band edges tend to produce particular responses of similar amplitude when excited by the same transient waveform. (3) If the waveform is altered by being passed through a filter with steep band edges and the response of that filter (the altered waveform) is applied to the input of a second filter that also possesses steep band edges, the amplitudes of singularity and particular responses of the second filter will depend on the overlap of the passbands of the two filters. If the passbands coincide, the amplitude of response of the second filter to the altered waveform will be similar to the amplitude of its response to the original waveform. If the passbands do not overlap, the amplitude of the response of the second filter will be greatly

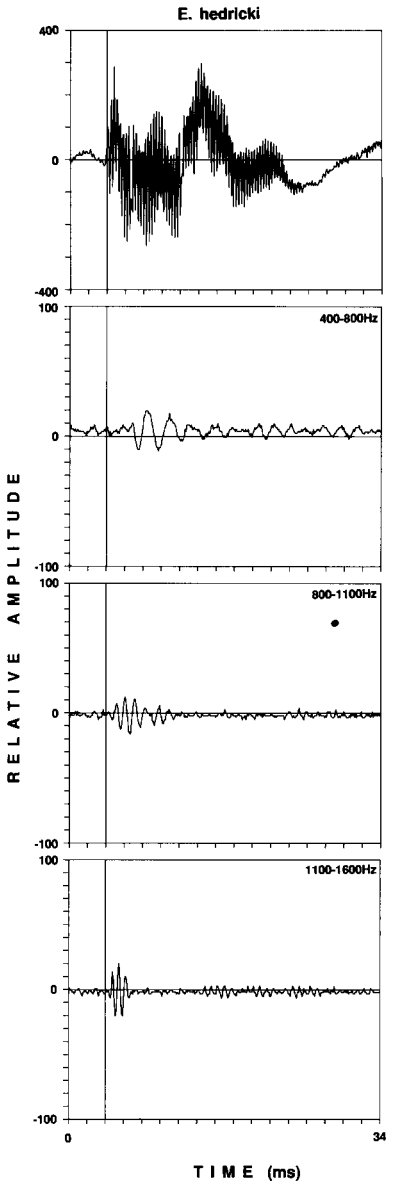

Fig. 10. Spectrographic analysis of an advertisement call of *E. hedricki*, showing singularity responses to the call onset

reduced. On the basis of these properties and the steepnesses of the band edges of our 16-pole analog filters, we have given spectral interpretations to our call analyses.

Examples of the filter outputs used in the call-analyses are shown in Fig. 9 for 3 species and in Fig. 10 for another. The top trace in each case is the unfiltered call, as captured by the digitizing oscilloscope. The highest-frequency components of the call of *E. brittoni* were above the oscilloscope's sampling frequency and therefore were not captured accurately (they were aliased). Beneath the displays of the unfiltered calls, and synchronized precisely to them, are displays of the analog-filter outputs. When we analyzed displays such as these, conspicuous components of the filter output that appeared consistently in the same phase of the unfiltered calls were taken to be responses to those calls. Thus, for example, spikes did not appear consistently in the 800–1100 Hz and 1100–1600 Hz filter outputs for the

Table 3. Transient spectrographic analysis of recorded calls of 8 Puerto Rican members of the genus *Eleutherodactylus*. Each entry is the average ratio (to the nearest 5 dB) of the peak of largest, consistently appearing response component from each filter to the peak amplitude of the unfiltered call. Blanks correspond to filters in which the response component was too small to be separated from the background noise (which typically was in the neighborhood of −40 dB re the peak amplitude of the unfiltered call)

PASS BAND	100–200 Hz	200–400 Hz	400–800 Hz	0.8–1.1 kHz	1.1–1.6 kHz	Dominant Frequencies (kHz)[1]
SPECIES	Regions A and B		Caudal Extension			
antillensis	−30 dB	−30 dB	−30 dB	−35 dB	−20 dB	1.8–2.2 2.5–3.6
brittoni	−10 dB	−10 dB	−10 dB	–	–	4.5–6.0
cooki	−15 dB	−25 dB	−30 dB	−25 dB	−10 dB	1.5–1.8
coqui	–	–	−30 dB	−10 dB	0 dB	1.2–1.9 1.6–3.5
hedricki	−10 dB	−15 dB	−25 dB	−25 dB	−25 dB	2.9–3.4
portoricensis	–	–	–	−20 dB	−15 dB	1.5–1.8 2.2–3.0
richmondi	–	0 dB	−10 dB	–	–	3.0–5.0
wightmanae	–	–	–	–	–	2.2–2.5 3.3–4.0

[1] Taken from Drewry and Rand (1983)

E. brittoni call. Therefore, those at the left hand edges of the displays for those filters in Fig. 9 were not taken to be responses to the call. The small transients in the 200–400 Hz, the 400–800 Hz, and the 800–1100 Hz filter outputs for *E. cooki* did appear consistently (in every one of 36 analyzed calls) and therefore were taken to be responses. The analyses are summarized in Table 3, which shows for each filter and each call the ratio (to the nearest 5 dB) of the peak amplitude of the filtered response to the peak amplitude of the unfiltered call. The right-hand column shows the dominant frequencies of the calls, as determined by previous spectrographic analysis and published by Drewry and Rand (1983).

Discussion

Caudal extension

Based on serial sections viewed with a light microscope, Wever (1985) divided the hair cells of the frog AP into 4 groups: 1) those connected to the "anterior tectorial body," 2) those connected to the "sensing membrane," 3) those that are "free standing," and 4) those connected to the "posterior tectorial body". His hair-cell counts for these groups (labeled ATB, SM, FS, and PTB, respectively) in 20 anuran species (all of the anuran species for which both Wever and we had hair-cell counts) are displayed in Table 2. Wever's "sensing membrane" is, at least in part, the structure we have described as a diaphragm; it also has been called the tectorial curtain (Wever 1973; Lewis 1977). We have not found evidence of hair cells connected directly to the diaphragm in any anuran AP we have examined, nor have we found any hair cells that are free standing (i.e., not connected to or surrounded by tectorial membrane). Viewing the tectorial membrane after it had been dehydrated, embedded in a nonaqueous medium, and sectioned, Wever had an image of it that was distinctly different from ours. When we treated this notoriously fragile membrane in a similar fashion, it always exhibited severe shrinkage and distortion. Comparing our hair cell counts with his, we conclude that his first group (connected to the anterior tectorial body) often corresponds closely to the population in region A, and that the combination of his other 3 groups often corresponds closely to the combined populations of region B and the caudal extension; but that none of his groups corresponds precisely either to our population B or to our population C. In fact, the correspondences between our B and C groups and his groups clearly vary from species to species. In general, our total hair cell count for each species was very close to his.

The trends evident in Fig. 5 imply that increased proportion of AP hair cells in the caudal extension is a derived trait that is exaggerated in the Puerto Rican *Eleutherodactylus* frogs. Thus we are led to two questions: What selective advantages might the caudal extension provide in general for anurans? Why is there so much diversity in that structure in these Puerto Rican frogs?

One possible selective advantage of the caudal extension is extension of the AP frequency range. In *Bombina bombina,* which has an extremely short caudal extension (C/A = 0.3; C/B = 0.2), the AP BEFs extend to 700 Hz (Hillery and Narins 1987). In *Rana catesbeiana* (C/A = 2.1; C/B = 1.4) the AP BEFs extend to 1000 Hz. Thus the presence of the caudal extension may have allowed the ranids (often considered to be typical modern frogs) to extend the frequency range of the AP by approximately 1/2 octave over that of the discoglossids (often considered to be among the most ancient living frogs). The actual range of BEFs in the *R. catesbeiana* caudal extension, however, is approximately 450 Hz to 1000 Hz (1.1 octaves) (Lewis et al. 1982b); so, in that species, it covers more than 1/2 octave of frequency range that already was available before it arose. This suggests the presence of selective advantages in addition to frequency-range extension.

In *E. coqui* (C/A = 2.6–3.9; C/B = 2.2–3.4) the AP BEFs extend to 1.4 kHz (Narins and Capranica 1976). If this were simply a matter of increase in the number of caudal extension hair cells, however, and if the sexual dimorphism suggested by our limited data were true, then one would expect the female *E. coqui*

(C/A = 3.6–3.9; C/B = 3.3–3.4) to have considerably greater range of AP BEFs than the male (C/A = 2.6–3.0; C/B = 2.2–2.6). In both sexes, the range of BEFs for the AP extends to approximately 1400 Hz. This suggests that the same midfrequency range is covered by a proportion of hair cells that is conspicuously greater in the female *E. coqui* than in the male. What advantage could this provide?

One possibility is increased resolution in the VIIIth nerve representation of sounds in the midfrequency range. One might think of the patterns of activity in the auditory periphery as a succession of dynamic images of the sound impinging on the frog's ear. For the amphibian papilla, the first of these images could be represented by the distribution of mechanical activity over the papillar surface. This would be translated by the transduction process to a second image, represented by the distribution of hair-cell excitation over the papilla. This hair-cell image evidently is quantized, with each hair-cell carrying one element (analogous to a pixel). Derived from the hair-cell image is a third image, which is represented by the pattern of spike activity over the axons of the amphibian-papillar branch of the VIIIth-nerve. Each axon carries an element of this VIIIth-nerve image. The tonotopy observed along the long axis of the *R. catesbeiana* AP and strongly inferred for other species (Lewis 1977; Lewis et al. 1982b) as well as that observed in the VIIIth nerve[3] suggests that one coordinate of all 3 images is frequency. To date, the variable or variables (if any) represented along the transverse AP axis have not been identified. There is an obvious variation of hair bundle morphology along that axis, but not along the axis tonotopy (Lewis 1976). AP axons exhibit marked variations in sensitivity (thresholds ranging over 40 dB or more) (Shofner and Feng 1981; Wilczynski et al. 1984; Stiebler and Narins 1990) and marked variations in adaptation dynamics (Megela and Capranica 1981; Megela 1984). Thus candidates for other coordinates for the hair-cell and VIIIth-nerve images are amplitude (mapped by variation in sensitivity) and temporal structure (mapped by variation in adaptation dynamics). Increasing the number of hair cells covering the same range of BEFs could increase the resolution of the hair-cell image over any of these coordinates. Preservation of that resolution in the translation to an VIIIth-nerve image would depend on the convergence of the innervation. If all synapses from hair cells to afferent axons are excitatory, convergence of signals from several hair cells (i.e., several elements of the hair-cell image) onto one axon (producing one element of the VIIIth-nerve image) would yield reduction of resolution.

To date, the only evidence regarding AP innervation patterns comes from ranid frogs. In the AP of *R. catesbeiana*, dye injection studies indicated that most of the afferent axons innervating the caudal extension contact from one to 3 hair cells, while most of those innervating region A contact from 6 to 15 hair cells (Lewis et al. 1982b). Thus, in *R. catesbeiana*, the innervation of the caudal extension seems to favor high resolution in the translation from hair-cell image to VIIIth-nerve image. Recent data from *R. pipiens pipiens* are entirely consistent with these findings from *R. catesbeiana* (Simmons et al. 1992).

With any of the candidate coordinates, increasing the resolution of the auditory image will increase the ability of the listener to discriminate acoustic signals from one another and from acoustic noise. Thus, in anurans with well-developed caudal extensions, one might expect greater discriminability for acoustic signals in the frequency range of that structure (approx. 450 to 1000 Hz or more) than in the frequency range of region A (approx. 100 to 300 Hz). The two published tests of this expectation that we know about are studies of frequency selectivity in *Hyla cinerea* (C/A = 1.6; C/B = 1.2) and *R. catesbeiana* (C/A = 1.9; C/B = 1.5) (Moss and Megela-Simmons 1986; Megela-Simmons 1988). Those studies show conspicuously greater ability of the animals to discriminate pure tones from acoustic noise in the frequency range of the caudal extension.

An alternative selective advantage of increased hair-cell numbers in the caudal extension is increased midfrequency sensitivity. If neighboring hair cells exhibited essentially the same stimulus-response properties, then neither increasing the total number of hair cells nor reducing the number of hair cells innervated by each afferent axon would lead to increased image resolution. They would lead instead to larger numbers of axons per element of the image. Rather than enhancing discrimination of acoustic signals from one another and from acoustic noise, this would enhance the ability of the listener to separate acoustic signals or acoustic noise from noise generated locally within the ear (e.g., channel noise in the hair cell). Thus it would enhance the absolute sensitivity of hearing. Based on this hypothesis, in the modern frogs one would expect greater absolute sensitivity over the frequency range of the caudal extension than over the frequency range of region A. This expectation is met in neural and behavioral audiograms of *R. catesbeiana* and *H. cinerea* (Lombard et al. 1981; Megela et al. 1985) and in neural audiograms of other modern frogs (Straughan 1975; Wever 1985). There typically are two sensitivity peaks – one in the high-frequency (basilar-papillar) range, the other in the midfrequency (caudal-extension) range. Regarding the midfrequency range, one can interpret these results in at least two ways: (1) The high midfrequency sensitivity in modern frogs is a consequence of the increased size of the caudal extension. (2) The high midfrequency sensitivity is inherent in the structures of the frog middle- and outer-ears; and this inherently-high sensitivity enhances the selective value of increased acoustic image resolution or further increased sensitivity brought about by increased size of the caudal extension.

In terms of the proportion of AP hair cells in the caudal extension, we find more diversity among 8 species of one genus on one island than we do among 58 other anuran species from around the world. The fact that the habitats of these 8 species overlap and that (according to

[3] The AP axons tend to remain together in the VIIIth nerve. Those with lower-frequency BEFs tend to be ventrad of those with higher-frequency BEFs

Table 4a. Spectrographic analysis from Table 3, with species listed in order of increasing average value of C/A

PASS BAND	100–200 Hz	200–400 Hz	400–800 Hz	0.8–1.1 kHz	1.1–1.6 kHz	Average C/A
SPECIES	Regions A and B		Caudal Extension			
hedricki	−10 dB	−15 dB	−25 dB	−25 dB	−25 dB	1.3
brittoni	−10 dB	−10 dB	−10 dB	−	−	1.4
wightmanae	−	−	−	−	−	2.0
cooki	−15 dB	−25 dB	−30 dB	−25 dB	−10 dB	2.2
portoricensis	−	−	−	−20 dB	−15 dB	2.2
antillensis	−30 dB	−30 dB	−30 dB	−35 dB	−20 dB	2.6
richmondi	−	0 dB	−10 dB	−	−	2.8
coqui	−	−	−30 dB	−10 dB	0 dB	2.8♂ 3.8♀

Table 4b. Spectrographic data from Table 4a, with all entries < −20 dB removed

PASS BAND	100–200 Hz	200–400 Hz	400–800 Hz	0.8–1.1 kHz	1.1–1.6 kHz	Average C/A
SPECIES	Regions A and B		Caudal Extension			
hedricki	−10 dB	−15 dB	−	−	−	1.3
brittoni	−10 dB	−10 dB	−10 dB	−	−	1.4
wightmanae	−	−	−	−	−	2.0
cooki	−15 dB	−	−	−	−10 dB	2.2
portoricensis	−	−	−	−20 dB	−15 dB	2.2
antillensis	−	−	−	−	−20 dB	2.6
richmondi	−	0 dB	−10 dB	−	−	2.8
coqui	−	−	−	−10 dB	0 dB	2.8♂ 3.8♀

the data in Table 3) the male advertisement calls of seven of them have components in the frequency range of the caudal extension suggests that call discrimination may have been a factor in the selective pressures sculpting that part of the AP in these species.

Some of the relationships between the data in Tables 1 and 3 support this conclusion. Restructuring Table 3 by placing the 8 species in order of increasing magnitude of C/A (calculated from Table 1), one obtains Table 4a. The calls of species with low C/A ratios *(E. hedricki, E. brittoni)* have strong spectral components in the frequency ranges of regions A and B but not in the higher-frequency ranges of the caudal extension. Calls of species with high C/A ratios *(E. cooki, E. portoricensis, E. antillensis, E. coqui)* have their stronger spectral components in the higher-frequency ranges of the caudal extension. This trend is more conspicuous in Table 4b, where components with relative amplitudes less than −20 dB have been omitted.

Although a high proportion of caudal-extension hair cells appears to be a derived feature, it does not follow that the highest proportions among PR *Eleutherodactylus* frogs are more derived than the lowest. If some or all of the PR *Eleutherodactylus* frogs shared a common ancestor, it could well have possessed a proportion of intermediate magnitude. Selective pressures then could have led to increases in some species, reductions in others.

Tectorial membrane and tuning

With the discovery of second-order electrochemical resonances in basilar-papilla hair cells in situ in the turtle *(Pseudemys scripta)* (Crawford and Fettiplace 1981), it has become popular to attribute frequency selectivity in auditory sensors of lower vertebrates in general to such resonances. This notion was reinforced for the frog AP by the discovery of second-order electrochemical resonances in the hair cells of regions A and B in *Rana temporaria* (Pitchford and Ashmore 1987). If the tuning that leads to variations in BEF and to tonotopy is accomplished by the second-order resonances in the individual hair cells, then the principal function of the mechanical elements of the ear would be coupling sound energy to the hair cells. Wever (1973) attributed just this function to the tectorial membrane; stating that the two layers of channels serve as a two-stage mechanical transformer, matching the impedance of the fluid (endolymph) of the ear to that of the hair bundle. This conjecture was not accompanied by any physical theory or analysis; and it seems to arise from the notion that the acoustic impedance of the fluid somehow plays a role in sound transmission in the ear. This notion was presented in the book by Wever and Lawrence (1954) in the idea that the combination of tympanum and ossicular chain matched the acoustic impedance of the air to that of the fluid of the ear; and it occasionally has emerged in more recent literature. Most modern theorists agree, however, that the compressibility of the fluid has virtually no effect on the operation of the ear – i.e., that the fluid behaves as though it were incompressible (Lesser and Berkley 1972; Allen 1977). Thus the wave properties (including the acoustic or distributed-parameter impedance) of the fluid play no role in inner-ear mechanics. This point of view is easily supported with physical models (e.g., compare the acoustic wavelength in water to the dimensions of the

inner ear). The fluid is merely one of several mechanical elements in the acoustic network of the inner ear, and if the middle ear provides impedance matching (a thoroughly reasonable hypothesis), it would be between the air and this entire network.

It is difficult to believe that the selective advantage of a structure as elaborate and highly organized as the frog AP tectorial membrane is simply its ability to transfer acoustic energy from the fluid in the papillar chamber to the hair cells. Furthermore, when second-order resonances were observed in AP hair cells, the tectorial membrane had been removed. When the tectorial membrane is in place, and the AP is intact, dynamics of AP tuning (as seen through individual AP afferent axons) are of order much greater than two (Lewis et al. 1991; Yu et al. 1991). In other words, there are major qualitative differences in the tuning behavior of the frog AP before and after the tectorial membrane is removed. Rather than simply acting as a conduit for acoustic energy, the tectorial membrane plays a role in frequency selectivity in that organ.

How it plays that role has been a subject of considerable speculation (Lewis and Leverenz 1983; Shofner and Feng 1983, 1984; Hillery and Narins 1984; Lewis and Lombard 1988). It evidently is firmly connected to the hair bundles, via a bulbous specialization at the tip of each kinocilium (Hillman 1969), a connection occurring on one side of the rim of the channel associated with each hair cell (Lewis 1976). The bundles behave, at least in part, as stiff elastic elements (Flock et al. 1977). Furthermore, there now is direct evidence of transduction from electrochemical variations in the hair cell to mechanical motion of the hair bundle (Crawford and Fettiplace 1985; Howard and Hudspeth 1987; Denk and Webb 1989). Combined with the well-established transduction to electrochemical variations in the hair cell from mechanical motion of the hair bundle (Hudspeth and Corey 1977), this implies that the electrochemical elements of the hair cell are connected bidirectionally to the mechanical elements of the ear. Thus, the tectorial membrane is connected not only to the elastic impedance of the hair bundle, but also to the electrochemical impedance of the hair cell (through what amounts to a bidirectional electromechanical transducer). Electrochemical and mechanical elements are combined, interactively, in a complex tuning structure. To this structure, the tectorial membrane itself may contribute some sort of distributed or lumped network of masses, elastic elements, and viscous resistances. The presence of two-tone suppression in region B and absence of two-tone suppression in the neobatrachian caudal extension may be related to hair-cell polarization (longitudinal in region B, transverse in the caudal extension) and the presumedly concomitant motion of the tectorial membrane. This may be a clue to the organization of the tuning structure.

Unfortunately, no direct observations of micromechanics of the AP tectorium or hair bundles have been published; and so far, no micromechanical model has been presented that takes into account all of the interacting electrochemical and mechanical elements. There is not even a micromechanical model addressing the role or roles of one of the most conspicuous features of the tectorial membrane – its system of channels. For another of its conspicuous features – the diaphragm – Wever's (1973) hypothesis that it intercepts the motion of the fluid in the AP chamber and transfers it to the tectorial membrane seems very reasonable. Between that point of interception and the spike-initiation locus of the primary afferent axon lies an intriguing and challenging network of electrochemical and mechanical elements.

Acknowledgements. The research reported here was supported by NIH Grants DC00112 (Lewis and Hecht) and DC 00222 (Narins) and by research travel grants from the Committees on Research at the University of California Berkeley and Los Angeles campuses. The authors are most grateful for the support and assistance provided to us by Dr. Robert Waide, Alejo Estrada and others at the El Verde Field Research Station of the Center for Energy and Environmental Research, San Juan, Puerto Rico. The authors also are grateful to Dr. M.M. Stewart for providing two of the animals used in the study and to Dr. Jacob Bastacky for support with the scanning electron microscopy. The AMRay 1000A SEM used for this study is supported in part by the Office of Health Research of the U.S. Department of Energy under contract DE-AC03-76SF00098 and in part by NIH Grant HL40521-01.

References

Allen JB (1977) Two-dimensional cochlear fluid model: new results. J Acoust Soc Am 61:110–119

Capranica RR (1976) Morphology and physiology of the auditory system. In: Llinás R, Precht W (eds) Frog neurobiology. Springer Berlin New York Heidelberg pp 551–575

Capranica RR, Moffat AJM (1974a) Excitation, inhibition and disinhibition in the inner ear of the toad *(Bufo)*. J Acoust Soc Am 55:480S

Capranica RR, Moffat AJM (1974b) Sensory processing in the peripheral auditory system of treefrogs *(Hyla)*. J Acoust Soc Am 55:480S

Capranica RR, Moffat AJM (1975) Selectivity of the peripheral auditory system of spadefoot toads *(Scaphiopus couchi)* for sound of biological significance. J Comp Physiol 100:231–249

Capranica RR, Frishkopf LS, Nevo E (1973) Encoding of geographical dialects in the auditory system of the cricket frog. Science 182:1272–1275

Cohen L (1989) Time-frequency distributions – a review. Proc IEEE 77:941–981

Crawford AC, Fettiplace R (1981) An electrical tuning mechanism in turtle cochlear hair cells. J Physiol 312:377–412

Crawford AC, Fettiplace R (1985) The mechanical properties of ciliary bundles of turtle cochlear hair cells. J Physiol 364:359–379

Denk W, Webb WW (1989) Simultaneous recording of fluctuations of hair bundle deflection and intracellular voltage in saccular hair cells. In: Wilson JP, Kemp DT (eds) Cochlear mechanisms. Plenum, New York, pp 125–133

Drewry GE, Rand AS (1983) Characteristics of an acoustic community: Puerto Rican frogs of the genus *Eleutherodactylus*. Copeia 1983:941–953

Duellman WE (1975) On the classification of frogs. Occ Pap Univ Kansas Mus Nat Hist 42:1–17

Duellman WE, Trueb L (1986) The biology of amphibians. McGraw-Hill, New York

Feng AS, Narins PM, Capranica RR (1975) Three populations of primary auditory fibers in the bullfrog *(Rana catesbeiana)*: their peripheral origins and frequency sensitivities. J Comp Physiol 100:221–229

Flock Å (1965) Transducing mechanisms in the lateral line canal organ receptors. In: Symposia on Quantitative Biology, Vol.

XXX, Cold Spring Harbor Laboratory of Quantitative Biology, Cold Spring Harbor, New York, pp 133–145
Flock Å, Flock B, Murray E (1977) Studies on the sensory hairs of receptor cells in the inner ear. Acta Otolaryngol 83:85–91
Frishkopf LS, Geisler CD (1966) Peripheral origin of auditory responses recorded from the eighth nerve of the bullfrog. J Acoust Soc Am 40:469–472
Frishkopf LS, Goldstein MH (1963) Responses to acoustic stimuli from single units in the eighth nerve of the bullfrog. J Acoust Soc Am 35:1219–1228
Geisler CD, van Bergeijk WA, Frishkopf LS (1964) The inner ear of the bullfrog. J Morphol 114:43–58
Hanken J (1989) Development and evolution in amphibians. Am Sci 77:336–343
Hillery CM, Narins PM (1984) Neurophysiological evidence for a traveling wave in the amphibian inner ear. Science 225:1037–1039
Hillery CM, Narins PM (1987) Frequency and time domain comparison of low-frequency auditory fiber responses in two anuran amphibians. Hearing Res 25:233–248
Hillman DE (1969) New ultrastructural findings regarding a vestibular ciliary apparatus and its possible functional significance. Brain Res 13:407–412
Howard J, Hudspeth AJ (1987) Brownian motion of hair bundles from the frog's inner ear. Biophys J 51:203a
Hudspeth AJ, Corey DP (1977) Sensitivity, polarity and conductance changes in the response of vertebrate hair cells to controlled mechanical stimuli. Proc Natl Acad Sci USA 74:2407–2411
Lesser MB, Berkley DA (1972) Fluid mechanics of the cochlea. Part 1. J Fluid Mech 51:497–512
Lewis ER (1976) Surface morphology of the bullfrog amphibian papilla. Brain Behav Evol 13:196–215
Lewis ER (1977) Structural correlates of function in the anuran amphibian papilla. Scan Electr Micr 1977(II):429–436
Lewis ER (1981) Suggested evolution of tonotopic organization in the frog amphibian papilla. Neurosci Lett 21:131–136
Lewis ER (1984) On the frog amphibian papilla. Scan Electr Microsc 1984:1899–1913
Lewis ER, Leverenz EL (1983) Morphological basis for tonotopy in the anuran amphibian papilla. Scan Electr Micr 1983:189–200
Lewis ER, Lombard RE (1988) The amphibian inner ear. In: Fritsch B (ed) The Evolution of the Amphibian Auditory System. Wiley, New York, pp 93–123
Lewis ER, Baird RA, Leverenz EL, Koyama H (1982a) Inner ear: dye injection reveals peripheral origins of specific sensitivities. Science 215:1641–1643
Lewis ER, Leverenz EL, Koyama H (1982b) The tonotopic organization of the bullfrog amphibian papilla, an auditory organ lacking a basilar membrane. J Comp Physiol 145:437–445
Lewis ER, Sneary MG, Yu X (1991) Further evidence for tuning mechanisms of high dynamic order in lower vertebrates. In: Dallos P, Geisler CD, Matthews JW, Ruggero MA, Steele CR (eds) The mechanics and biophysics of hearing. Springer, Berlin Heidelberg New York, pp 139–146
Lombard RE, Fay RR, Werner YL (1981) Underwater hearing in the frog, *Rana catesbeiana*. J Exp Biol 91:57–71
Lowenstein O, Wersäll J (1959) A functional interpretation of the electron microscopic structure of the sensory hairs in the cristae of the elasmobranch *(Raja clavata)* in terms of directional sensitivity. Nature 184:1807–1808
Lynch JD (1971) Evolutonary relationships, osteology, and zoogeography of leptodactylid frogs. Univ Kansas Mus Nat Hist Misc Publ 53:1–238
Lynch JD, Myers CW (1983) Frogs of the *fitzingeri* group of *Eleutherodactylus* in eastern Panama and Chocoan South America (Leptodactylidae). Bull Am Mus Nat Hist 175:481–572
Megela AL (1984) Diversity of adaptation patterns in responses of eighth nerve fibers in the bullfrog, *Rana catesbeiana*. J Acoust Soc Am 75:1155–1162
Megela AL, Capranica RR (1981) Response patterns to tone bursts in peripheral auditory system of anurans. J Neurophysiol 46:465–478
Megela-Simmons A (1988) Masking patterns in the bullfrog *(Rana catesbeiana)*. I: Behavioral effects. J Acoust Soc Am 83:1087–1092
Moss CF, Megela-Simmons A (1986) Frequency selectivity of hearing in the green treefrog, *Hyla cinerea*. J Comp Physiol A 159:257–266
Megela-Simmons A, Moss CF, Daniel KM (1985) Behavioral audiograms of the bullfrog *(Rana catesbeiana)* and the green treefrog *(Hyla cinerea)*. J Acoust Soc Am 78:1236–1244
Narins PM, Capranica RR (1976) Sexual differences in the auditory system of the tree frog *Eleutherodactylus coqui*. Science 192:378–380
Pitchford S, Ashmore JF (1987) An electrical resonance in hair cells of the amphibian papilla of the frog *Rana temporaria*. Hearing Res 27:75–84
Retzius G (1881) Das Gehörorgan der Wirbeltiere; Morphologische und histologische Studien. I. Das Gehörorgan der Fische und Amphibien. Samson and Wallin, Stockholm
Rivero JA (1978) Los Anfibios y Reptiles de Puerto Rico. San Juan: Editorial Universitaria, Universidad de Puerto Rico, pp 3–42
Sachs MB (1964) Responses to acoustic stimuli from single units in the eighth nerve of the green frog. J Acoust Soc Am 36:1956–1958
Schwartz A, Henderson RW (1985) A guide to the identification of the amphibians and reptiles of the West Indies exclusive of Hispaniola. Milwaukee Public Museum, Milwaukee, pp 8–25
Shofner WP, Feng AS (1981) Post-metamorphic development of the frequency selectivities and sensitivities of the peripheral auditory system of the bullfrog, *Rana catesbeiana*. J Exp Biol 93:181–196
Shofner WP, Feng AS (1983) A quantitative light microscopic study of the bullfrog amphibian papilla tectorium: correlation with tonotopic organization. Hearing Res 11:103–116
Simmons DD, Bertolotto C, Narins PM (1992) Innervation of the amphibian and basilar papillae in the leopard frog: reconstruction of single labeled fibers. J Comp Neurol, in press
Stiebler IB, Narins PM (1990) Temperature-dependence of auditory nerve response properties in the frog. Hearing Res 46:63–82
Straughan IR (1975) An analysis of the mechanisms of mating call discrimination in the frogs *Hyla regilla* and *H. cadaverina*. Copeia 1975(3):415–424
Wever EG (1973) The ear and hearing in the frog, *Rana pipiens*. J Morphol 141:461–478
Wever EG (1985) The amphibian ear. Princeton Univ Press, Princeton, pp 1–488
Wever EG, Lawrence M (1954) Physiological acoustics. Princeton Univ Press, Princeton, pp 1–454
Wilczynski W, Zakon HH, Brenowitz EA (1984) Acoustic communication in spring peepers. J Comp Physiol A 155:577–584
Yen N (1987) Time and frequency representations of acoustic signals by means of the Wigner distribution function: Implementation and interpretation. J Acoust Soc Am 81:1841–1850
Yu X, Lewis ER, Feld D (1991) Seismic and auditory tuning curves from bullfrog saccular and amphibian papillar axons. J Comp Physiol A 169:241–248
Zakon HH, Wilczynski W (1988) Anuran eighth nerve physiology. In: Fritzsch B (ed) The evolution of the amphibian auditory system. Wiley, New York, pp 125–155